



# Changing Snow Water Storage in Natural Snow Reservoirs

Christina Marie Aragon<sup>1</sup> and David F. Hill<sup>2</sup>

<sup>1</sup>Oregon State University, Water Resources Engineering, Corvallis, OR, 97331, USA

<sup>2</sup>Oregon State University, Civil and Construction Engineering, Corvallis, OR, 97331, USA

**Correspondence:** Christina Marie Aragon (aragonch@oregonstate.edu)

**Abstract.** This work defines a new snow metric, snow water storage (SwS), which is the integrated area under the snow water equivalent (SWE) curve. Other widely-used snow metrics capture snow variables at a single point in time (e.g. maximum SWE) or describe temporal snow qualities (e.g. length of snow season), SwS can be applied at numerous spatial and temporal scales. The flexibility in the SwS metric allows us to characterize the natural reservoir function of snowpacks and quantify how this function has changed in recent decades. In this study, changes in the SwS metric are evaluated at point, gridded and aggregated scales across the conterminous United States (hereafter US). There is special focus on 16 mountainous EPA Level III Ecoregions (ER3s), which play an inordinate role in US annual SwS ( $SwS_A$ ). An average of 72% of the annual  $SwS_A$  in the US is held in the 16 mountain ER3s, despite these ER3s only covering 16% of the US land area.  $SwS_A$  and monthly SwS ( $SwS_M$ ) have changed significantly across the US since 1982 at point, gridded and ER3 scales. This change is spatially variable across the US with more spatially widespread significant decreases in  $SwS_A$  than increases. The greatest  $SwS_M$  loss occurs early in the snow season, particularly in November. All but two ER3 mountain ranges have decreasing trends in  $SwS_A$  and there has been a 22% decline in  $SwS_A$  across all mountain ER3s. Unsurprisingly, the highest elevations are responsible for the greatest SwS in all mountain ranges, though the elevations that have lost or gained SwS over the 39 years of study are variable across mountain ranges. Comparisons of the percent change in SwS to other snow metrics reveals that change in the SWE curve has not been shape-preserving - instead, the SWE curve has been flattening. As we move into a future of increased climate variability and increased variability in mountain snowpacks, spatially and temporally flexible snow metrics such as SwS may become more valuable.

## 1 Introduction

Seasonal snow is a keystone resource in mountainous regions and at high latitudes across the United States (US), providing an important ecosystem service by functioning as natural reservoirs at river headwaters. These snow reservoirs play a key role in the water cycle by storing water during the cool season and releasing water gradually throughout the warm season when human and ecological demand is the highest. Given the vulnerability of seasonal snow water storage to climate warming and the importance of snow-derived water to municipalities, agriculture, ecosystems, and hazard forecasters, it is vital to understand how water storage in our natural snow reservoirs is evolving in the context of a changing climate (Immerzeel et al., 2020; Sturm et al., 2017; Barnett et al., 2005; Li et al., 2017; Siirila-Woodburn et al., 2021). As the majority of natural snow water storage occurs in mountainous regions across the United States, it is vital to understand how the natural reservoir function



of snowpack is changing in individual mountain ranges. EPA Level III ecoregions (ER3s) delineate areas of similar abiotic and biotic (including humans) components of terrestrial and aquatic ecosystems that can be used for ecosystem management and to enhance environmental understanding. Numerous ER3s correspond to the major mountain regions that serve as the largest natural reservoirs in the country. This work will evaluate how snow water storage is changing in mountain ecoregions to increase the relevance of the findings to ecosystem and human-related impacts.

There are many snowpack characteristics of interest. These include snow depth (Hs), snow covered area (SCA), vertical structure or layering of the snowpack, and more. Snow water equivalent (SWE), the depth of water one would get upon melting a column of snow, is the snowpack characteristic that is most relevant for many water resources applications. Having an estimate of SWE across a watershed is analogous to having a reservoir elevation - it allows you to quantify the amount of water being stored that will become available as stream flow once the snowpack melts.

The metrics used to monitor changes in our snowpacks largely fall into two categories; they can be temporal snapshots that give us information about snow magnitude at a certain point in time, or they can provide information about snow timing (Nolin et al., 2021). Metrics that fall into the category of temporal snapshots include SWE observed at monitoring stations such as the snow telemetry (SNOTEL) and snow course networks operated by the Natural Resources Conservation Service (NRCS, Serreze et al. (1999)), snowpack volume on April 1st, spring SCA, the approximate date of peak SWE, and others. Previous studies have reported widespread and substantial declines in April 1st SWE across snow course and SNOTEL networks in the western US (Mote et al., 2018; Clow, 2010), declines in the April 1st SWE volume in California (Huning and AghaKouchak, 2018), and declines in spring SCA (Derksen and Brown, 2012) across the Northern Hemisphere.

Snow metrics that give us information about the timing of snow include snow cover duration (SCD), date of snow onset (DSO) and date of snow disappearance (DSD), among others. Multiple studies have reported widespread declines in SCD from regional to global scales (Bormann et al., 2018; Notarnicola, 2020; Choi et al., 2010) as well as a later DSO (Notarnicola, 2020) and an earlier DSD (Notarnicola, 2020). April 1st SWE has long been used in snow hydrology as an indicator measurement because it is approximately the date of peak snowfall in many locations and because it is relevant to snow course data, which has a very long period of record, but which is usually only collected at the start of each month. Though April 1st SWE has been effectively used as an indicator for the changing character of mountain snowpacks, it is a temporal snapshot that does not provide any information on snow stored during the rest of the season. Conversely, other snow metrics such as SCD, DSO or DSD give us information on snow timing, but do not provide insight on the amount of water held in mountain snowpacks. For example, trends in April 1st SWE could be a result of reduced or increased snow, temporal shifts in the snowpack, or increased variability (repeated accumulation and melt events) in the snowpack. In order to more completely understand how our snow water reservoirs are changing, we need to consider the full time-history of the accumulation and loss of the snow over the water year.

A conceptual SWE curve is shown in figure 1(a). Mountain snowpacks generally have a DSO, where the SWE starts the accumulation phase of the snow season up to a peak SWE ( $SWE_{max}$ ), which may or may not occur on Apr 1. After  $SWE_{max}$ , the ablation phase of the snow season starts and the SWE depth declines until it reaches zero at the DSD. The SCD is captured by the width of the SWE curve. Multiple factors can result in systematic changes to the shape of the SWE curve including



climate change (Lute et al., 2015), natural land cover change such as wildfire (Gleason et al., 2019) or beetle kill (Pugh and Small, 2012; Boon, 2007; Winkler et al., 2014) and man-made land cover change, such as forest thinning (Krogh et al., 2020; Sun et al., 2022) or logging (Winkler et al., 2005; Troendle and Reuss, 1997). The shaded regions in figure 1 provide examples  
65 of how the SWE curve may have changed from the past to present day. For example, a current SWE curve could be a scaled (reduced) version of a past SWE curve (figure 1(b)). This would result in a later DSO, a lower  $SWE_{max}$ , an earlier DSD and a shorter SCD.

Changes in SWE curves could also result from a temporal shift in the historic curve (figure 1(c)). This would not impact  $SWE_{max}$  or SCD, but metrics including April 1 SWE, DSO, and DSD would be affected. Figure 1(d) gives yet another example  
70 of a theoretical current scenario, compared to a historic one. In this case, the shape of the conceptual SWE curve is changed by repeated accumulation and melt events during the accumulation season. As shown in this illustration, metrics such as DSO, DSD, SCD,  $SWE_{max}$ , and April 1st SWE are all unchanged but it is clear that the snowpack is different than in the past. Previous literature has quantified increasing ablation during the accumulation period by defining a ‘melt fraction’ (Musselman et al., 2021) - the ratio of the melt that occurs during the accumulation phase to the total melt. Their metric helps to identify snow-  
75 packs that have considerable variance and demonstrate vulnerability to warming and rain-on-snow events. Another example of changing snowpack is shown in figure 1(e). Here, the  $SWE_{max}$  could remain constant in magnitude and timing, but the SCD could decrease due to a later DSO and earlier DSD. Finally, figure 1(f) shows a theoretical future in which DSO, DSD, SCD, April 1st SWE and  $SWE_{max}$  all remain constant, but it is clear that there is less snow present throughout the season.

In order to fully understand the nature by which snow water reservoirs are changing, we need to consider the full SWE curve,  
80 both in magnitude and in timing. This work aims to characterize the extent to which snowpacks serve as natural reservoirs and evaluate spatial and temporal changes in snow water storage in a new, integrated way. We first formalize the definition of SwS (snow water storage) as the time-integral of SWE over the water year. We note that SwS can be computed over a range of temporal scales (day, month, year). We also note that SwS can be evaluated at a single point (either a measurement station, or a model grid point), or can be spatially aggregated over an area of interest (specific watershed or other). We then look at trends  
85 in SwS in mountain snowpacks by addressing the following research questions: (1) Are there significant trends in monthly and annual SwS across the US at discrete point scales? (2) How do SwS aggregate over the ER3s associated with mountain areas? (3) How do changes in snow water storage vary as a function of elevation between mountainous ecoregions?

## 2 Methods

### 2.1 Snow Water Storage Metric (SwS)

90 This work defines a new snow metric, snow water storage (SwS). SwS quantifies the depth of water stored in snow reservoirs over time and is calculated by integrating the area under the SWE curve:

$$SwS = \int SWE(t) dt, \quad (1)$$



where SWE has dimensions of length, and integration occurs over a time period (water year, a given month, etc.) of interest. If daily SWE data are used for this calculation at a given point (say a SNOTEL site), SwS therefore has dimensions of meter-days, or md.

As defined above, SwS is a quantity computed at a single point, e.g. a SNOTEL location, or at the center of a model grid cell. However, the SwS metric can also be aggregated across various spatial scales. There are numerous re-analysis products that provide spatially-distributed SWE information on a regular grid. In this case, SwS can be computed for a horizontal area (say a particular watershed) of interest. In this case, the dimensions of SwS will be  $m^3d$ . Ultimately, this integrated metric helps us to understand how much water is held in our snow reservoirs and for how long.

SwS can also be computed for various integration periods. If the integration is done over the entire water year, this yields annual SwS ( $SwS_A$ ). In the integration is for a particular month, this yields monthly SwS ( $SwS_M$ ). Integrating daily SWE data over a single day produces the daily value of SwS ( $SwS_D$ ), but this is simply is the same as daily SWE.

## 2.2 Data

Datasets used for this paper are summarized in Table 1, and briefly reviewed here. Daily observations of SWE were obtained from Natural Resources Conservation Service SNOTEL stations (Serreze et al., 1999) and from Cooperator Snow Sensors (COOP). The SNOTEL network provides data at discrete scattered points across the western US and the COOP stations used in this study provide data across California. We used the 465 stations that have a period of record from at least water year 1982 to water year 2020 with less than 10% of days missing during that period.

This study also uses the University of Arizona SWE (UASWE) dataset (Zeng et al., 2018; Broxton et al., 2019) a daily 4-km gridded dataset that spans the US. The UASWE dataset assimilates SWE and snow depth observations into an empirical temperature index snow model that is forced with PRISM temperature and precipitation data (Daly et al., 2008). The primary value of this dataset is that it provides SWE estimates at locations other than the SNOTEL stations. This allows for the aggregation of SWE information over areas of interest (Zeng et al., 2018). While we recognize the potential limitations of using a modeled SWE product, the UASWE product has been shown to outperform (Dawson et al., 2018) other gridded SWE products such as the SWE estimates from the Snow Data Assimilation System (SNODAS, Center. (2004)). Additionally, a spatially-continuous, gridded product allows us to build a more complete picture of spatial changes in SwS and how changes in SwS are occurring at aggregated scales.

The EPA Level III Ecoregions (ER3s) (McMAHON et al., 2001; Omernik and Griffith, 2014), regions with similar ecosystems and environmental resources, were used to identify mountainous regions and to delineate the grid cells in the UASWE dataset that were associated with each ER3 (figure 2). Mountainous ER3s were included in this study if at least half of their area resided in the snow covered mask (described in section 2.3 below). Since each ER3 has similarities in biotic, abiotic, terrestrial and aquatic ecosystem components, examining SwS change in any given ecoregion may help us understand ecosystem impacts that are related to changes in SwS.



125 Finally, NASA SRTM Digital Elevation data (Farr et al., 2007) were re-gridded to create a digital elevation model (DEM) matching the grid of the UASWE product. Elevation data were used to calculate watershed hypsometry in each ER3. The procedure used to calculate a hypsometry grid is described in section 2.4.2.

Though the station and ER3 datasets extend beyond the conterminous US, the UASWE dataset does not. All datasets were spatially constrained to the conterminous US in order to facilitate the comparison of results between spacial scales.

### 130 2.3 Study Area

As noted above, this study considers both discrete station data that focus on the western US, and spatially-continuous gridded data that cover the conterminous US. Regarding the gridded data, many locations have little to no snow. Therefore, we restrict analysis of the gridded product to locations that have a mean of at least 30 snow covered days per year based on a 39-year climatology (1982-2021) (figure 3). As expected, snow cover duration increases with latitude and elevation, with the longest  
135 snow cover duration found along mountain tops in the western US. In the ER3 SwS change analysis, all ER3s are considered that contain grid cells that meet the 30-day snow cover threshold, though we more closely examine the mountainous ecoregions across the country since they store the bulk of our winter water.

## 2.4 Analysis

### 2.4.1 SwS Trends

140 To answer the first research question, are there significant trends in  $SwS_A$  and  $SwS_M$  across the US, these quantities were computed over a 39-year period of record (water years 1982-2020) at stations and at UASWE grid cells. The grid cell-based SWE from the UASWE product was additionally aggregated for each ER3 in order to assess trends at larger scales.

The Mann-Kendall test is a rank-based non-parametric test that is used to evaluate monotonic (increasing or decreasing) trends in temporally-varying data (Hirsch et al., 1982). Thus, the null hypothesis is that the data are randomly and independently  
145 ordered and the alternative hypothesis is that a monotonic trend exists in the data. Though the Mann-Kendall test is widely used in hydrological studies, it does not account for positive autocorrelation, which increases the probability of detecting trends when no trends exist. Because of this, many studies have turned to a modified Mann-Kendall test that does account for autocorrelation (Hamed and Rao, 1998). This study used the Hamed and Rao Modified MK test from the pyMannKendall python package to compute trends in SwS (Hussain and Mahmud, 2019).

### 150 2.4.2 SwS Trends in Mountain Ecoregions

Our analysis is focused on 16 ER3s that corresponding to mountain ranges that receive substantial snowfall relative to surrounding ecoregions. 12 of these ecoregions are located in the western US, and 4 ER3s are located in the Eastern US. The relative elevation of  $SwS_A$  change in each ER3 is examined in this study. In order to make trends in  $SwS_A$  comparable over the wide range of elevations across the US, the elevations of each ER3 are converted to hypsometry scores. Each ER3 boundary is  
155 used to select co-located elevation data from the regridded NASA SRTM Digital Elevation Dataset. ER3 hypsometry is calcu-



lated by determining the percentage of the ER3 area that falls below a given elevation within that ER3. Thus, there is 0% of the ER3 at the lowest elevation of the ER3 and 100% of the ER3 is below the highest elevation. In this work, each elevation grid cell in the DEM is turned into a value between 0 and 1 based on where that grid cell lies relative to other elevation grid cells within the same ER3. This procedure yields a gridded dataset of ER3 hypsometry scores for the US. Hypsometry scores in each mountain ER3 are binned into 10% increments, from 0% of an ER3 below to 100% of an ER3 below, in order to compute the mean  $SwS_A$  and the percent change in each hypsometry band from 1982-2020. The percent change in the interquartile range (IQR) of  $SwS_D$  was also computed for each hypsometry band from 1982-2020. To calculate the percent change in IQR, the IQR in each ER3 is calculated for each year in the study by subtracting the 25th percentile from the 7th percentile of  $SwS_D$  SWE. The trend is evaluated in each hypsometry band following the trend analysis described in section 2.4.1.

### 165 2.4.3 $SwS_A$ Compared to Other Snow Metrics

$SwS_A$  trends are compared to other commonly used snow metrics including April 1st SWE,  $SWE_{max}$ , day of  $SWE_{max}$ , and SCD in order to evaluate what type of information the  $SwS_A$  metric provides that other metrics do not. This is done in 3 ways using the station data. First, the percent of stations with positive, positive significant, negative and negative significant trends in each metric are computed. Second, a regression is computed between the percent change in  $SwS_A$  and each other metric above using empirical data from the stations. Third, the relationship between the percent changes in the empirical data is compared to what we would expect the relationship to be in a few conceptual SWE curve change scenarios presented in figure 1. For example, the empirical relationship between the percent change in  $SwS_A$  and the percent change in  $SWE_{max}$  is compared to what we would expect the percent change to be if there has been a uniform scaling in the conceptualized SWE curve as is depicted in 1b.

## 3 Results

### 175 3.1 SwS Trends

#### 3.1.1 $SwS_A$ Trends

Of the 97 SNOTEL and COOP stations with increasing trends in  $SwS_A$ , only 10 had significant ( $p < 0.1$ ) increases (figure 4). One hundred twenty three of the stations of the 367 stations with decreasing  $SwS_A$  trends, had significant decreases. Spatially, there are widespread decreasing  $SwS_A$  trends across most of the 11 western states that contain snow stations. The is a mean decline of 39.8% across the stations with significant declines in  $SwS_A$ , though these values range from a 17.3% decline to a 86.5% decline. The 10 stations with significant increases in  $SwS_A$  range from a 6.2% increase to a 78.4% increase, with a mean increase of 37.4%. The stations with increasing  $SwS_A$  trends are mostly located in the Northern and Middle Rockies and also includes a few station in the Southern Rockies and in the Cascades.

As we move from discrete station data to the the spatially-continuous gridded UASWE data, we find similar geographic patterns of significant changes in  $SwS_A$  in the western US (figure 5). This is not surprising given that the UASWE product assimilates SNOTEL (and other) data. The benefit of including a spatially distributed product such as UASWE in this analysis



is that it adds detail and insight as to where changes in  $SwS_A$  are occurring beyond the western US and in-between the locations where discrete stations are located. Remember that the station network only includes the western portion of the US. Significant increases in grid cell  $SwS_A$  are primarily found in the north-central and north-eastern US. Only 5% of US grid cells have significant increasing trends, and have a mean percent increase of 84.4%. From 1986-2015, these regions have experienced an increase in annual precipitation, particularly in spring and fall, though these regions also show spatially-variable increases during the winter (Easterling et al., 2017). These precipitation changes may partially explain the increases in  $SwS_A$ , though these regions have also experienced increases in winter temperatures over the same time period. Significant decreases in  $SwS_A$  are more widespread and are found across the western US, the Appalachian Mountains, the Blue Ridge Mountains and in the Ozarks. There is a mean decline of 43.5% across the 11% of US grid cells that have significant decreasing trends in  $SwS_A$ .

Figure 6 indicates the percent change in  $SwS_A$  across ER3s. Aggregating UASWE  $SwS_A$  at ER3 scales spatially-filters (and thus mutes) some of the grid cell-scale trends in  $SwS_A$  as can be seen when comparing figures 4 and 5. Of the 51 ER3s that are evaluated in this study, 37% have increasing trends and 63% have decreasing trends. Only one ER3 has a significant positive  $SwS_A$  trend of 85.8% increase while four ER3s have significant decreasing  $SwS_A$  trends, with a mean percent decrease of 47.4%. All four of the ER3 that have significant  $SwS_A$  trends are mountain ER3s. Of the 16 mountainous ecoregions (outlined in red), only one shows (insignificant) increases in  $SwS_A$ , while 15 ER3s show decreases in  $SwS_A$ . This means that 93.8% of mountain ER3s that play a role in snow water storage have declined from 1982-2020.

### 3.1.2 $SwS_M$ Trends

Figures 7, 8, and 9 summarize trends in  $SwS_M$  evaluated at stations, UASWE grid cells and ER3s, respectively. There are predominantly significant decreases in  $SwS_M$  occurring across all months at all spatial scales examined. November has the greatest number of stations with significant  $SwS_M$  loss at stations and grid cells and ER3 scales. November also has the greatest monthly median percent loss of  $SwS_M$  per decade at stations (14.1%) and grid cell (11%), though the greatest monthly median percent loss of  $SwS_M$  per decade in ER3s was in March (15.3%). The greatest number of stations with significant  $SwS_M$  increase occur in October, February, March and April at the station scale, and in February and March at the grid cell spatial scales, though there was an overall negative median percent change in  $SwS_M$  per decade during these months. At the grid-cell scale, October, March-May and July-August all have a 0 median percent change in  $SwS_M$  per decade. At the ER3 scale, April stands out as being the only month with a significant positive median percent change in  $SwS_M$  per decade (51.5%), though if you consider the mountain ER3s (where there is the highest  $SwS$ ), there is a significant negative median percent change of 15% per decade. This indicates that the large significant increases in April  $SwS_M$  are not occurring in mountainous parts of the country. Looking at only mountain ER3s, there are no months with a significant positive median percent change. ER3s have the greatest number of significant increase in  $SwS_M$  in October. October is also the only month that mountain ER3s had any significant increases. Most data points that indicate significant positive increases in monthly storage are considered outliers at all spatial scales.



### 3.2 SwS<sub>A</sub> Trends on the Landscape - Mountain ER3s

220 Analysis of mountain ERs illuminates the out-sized role mountains play in storing winter snow water resources as snowpack. An average of 72% of the annual SwS<sub>A</sub> in the US is held in the 16 mountain ER3s, despite these ER3s only covering 16% of the US land area. Further, an average of 65% of the annual SwS<sub>A</sub> in the US is held in western mountain ERs, which cover 12% of the US land surface. Across all mountain ER3s, there has been a 22% decline in SwS<sub>A</sub> over the 39 year period of study. Over the same time span, there has been a 24% decline in SwS<sub>A</sub> in western mountain ER3s, indicating that western snow reservoirs  
225 are shrinking faster than Eastern snow reservoirs.

Table 2 summarizes the fraction of US SwS<sub>A</sub> in each mountain ER3, the percent change in SwS<sub>A</sub> from water years 1982 to 2020, and the p-value associated with the percent change. Snowpack plays an important role in climate, ecological processes and recreation in both eastern and western mountains, but is essential to warm-season water resources in the western US. Snowpack is not essential to warm-season water resources in the Eastern US since there is adequate warm-season precipitation.  
230 In the western US, the Middle Rockies are responsible for the greatest fraction (11.6%) of SwS<sub>A</sub> in the country, followed by the Southern Rockies (9.8%) and the Idaho Batholith (8.3%). All mountain ER3s in the western US have declines in SwS<sub>A</sub> over the last 39 years with the exception of the North Cascades, where SwS<sub>A</sub> increased by 13%. The greatest declines in western SwS were in the Arizona/New Mexico Mountains (56% decline), the Eastern Cascade Slopes (40% decline) and Foothills and the Cascades (39% decline). Similar to the west, all eastern mountain ER3s showed declines in SwS<sub>A</sub> over the last 39 years  
235 with the exception of one. The Northeastern Highlands are responsible for the greatest fraction (3.5%) of SwS<sub>A</sub> in the in the Eastern US and had a SwS<sub>A</sub> increase of 13.15% over the last 39 years. The greatest decline in SwS<sub>A</sub> in the Eastern US was in the Ridge and Valley (11% decline), which holds an average of 0.2% of US SwS<sub>A</sub>.

All mountain ER3s have the greatest SwS<sub>A</sub> in the highest 10% of the ER3s that fall within their boundaries (figure 10). Most mountain ER3s have decreasing trends in SwS<sub>A</sub> across all hypsometry bins, though the Sierra Nevada, the Wasatch and Uinta  
240 Mountains, the Southern Rockies, the North Central Appalachians and the North Cascades show increasing trends in SwS<sub>A</sub> at low elevations with decreasing trends at higher elevations. The Northern Highlands is the only ER3 that shows increasing trends in SwS<sub>A</sub> at all elevations. Increasing trends in SwS<sub>A</sub> at low elevations in some ER3s may partially be a result of very low SwS<sub>A</sub> to begin with, thus small changes in SwS<sub>A</sub> may suggest large percent changes. Looking across all mountain ER3s, there are only significant declining SwS<sub>A</sub> trends and no significant increasing trends.

245 By looking at the percent change trends in the IQR of SwS<sub>D</sub>, we are able to get an idea of interannual SWE variability has changed from 1982-2020. Several ER3s have increases in the SwS<sub>D</sub> IQR of the lowest hypsometry bands, which correspond to the lowest parts of ER3s. This could be a result of increasing snow variability as freezing levels move to higher elevations, resulting in increased irregularity in precipitation form. In the middle and upper hypsometry bands of most ER3s, there is largely a decrease in the IQR. This may be a result of declining snowpacks, which would allow for less variability in the  
250 range of SwS<sub>D</sub> values overall. The Northern Highlands, Ridge and Valley, Central Appalachians and North Cascades stand out somewhat in that they have increasing trends in IQRs across most hypsometry bands.





### 3.3 SwS<sub>A</sub> Compared to Other Snow Metrics

The SwS<sub>A</sub> metric was compared to other commonly used snow metrics including the annual number of snow covered days, SWE<sub>max</sub>, day of SWE<sub>max</sub> and April 1st SWE. The fraction of increasing, decreasing and no trends in each of these metrics is summarized in Table 3. The percent of stations with negative trends was greater than the percent of stations with positive and positive significant trends in all metrics considered. Across all metrics, there was a relatively small (14%) range in the percent of stations with positive trends and only 1-2% of stations had significant positive trends across all metrics. There was an 18% range in the percent of stations with negative trends and a 14% range in the number of stations with significant positive trends across all metrics.

Figure 11 provides the results of regressing the percent change in April 1 SWE, SWE<sub>max</sub> and SCD on to the percent change in SwS<sub>A</sub> and the percent change of SCD onto SWE<sub>max</sub> using empirical station data. In all cases, the slope is less than 1 (although only slightly less in the case of April 1 SWE). The regression analysis between the percent change in SwS<sub>A</sub> and April 1 SWE yields a slope of 0.94. This nearly 1:1 relationship suggests that SwS<sub>A</sub> and April 1 SWE have experienced a similar percent change over the 39-year period of record. The regression between the percent change in SwS<sub>A</sub> and the percent change in SWE<sub>max</sub> yields a slope of 0.86, suggesting that the changes in SWE<sub>max</sub> have been slower than the changes in SwS<sub>A</sub>. With a slope of 0.26 in the SwS<sub>A</sub> versus SCD regression, we find that SwS<sub>A</sub> has changed about 4 times faster than SCDs. The regression analysis between the percent change in SWE<sub>max</sub> and SCD also yields a slope of 0.26. The percent change in April 1 SWE was nearly identical to the percent change in SWE<sub>max</sub>, with a slope of 1.03 when April 1 SWE was regressed onto SWE<sub>max</sub> (not pictured).

## 4 Discussion

The widespread losses of SwS<sub>A</sub> over the last 39 years reported in this study are consistent with the broader narrative of snowpack change literature, which has established declines in snow covered area, snow cover duration, April 1st SWE, SWE<sub>max</sub>, etc. Losses of winter snowpack are largely attributed to increasing global temperatures (Hamlet et al., 2005), which have resulted from a combination of natural variability and anthropogenic-caused climate warming (Rupp et al., 2013; Pederson et al., 2013). Though the majority of SwS trends are declining, there is notable temporal and spatial variability in this change. The declining trends in SwS<sub>A</sub> are a reflection of declining trends in SwS<sub>M</sub> in nearly every month, at every scale. The greatest SwS<sub>M</sub> losses occur early in the snow season, particularly in November. The loss of early season SwS is consistent with previous work that used satellite imagery and reported that that first snow is occurring later (Notarnicola, 2020). Although decreasing trends in SwS<sub>A</sub> dominate the US spatially, the north central plains and New England show increasing SwS<sub>A</sub> trends. Snowmelt and rain-on-snow are known to be flood generating mechanisms in New England, Minnesota and along the Mississippi and Missouri Rivers (Collins, 2009; Novotny and Stefan, 2007; Wiel et al., 2018; Olsen et al., 1999). The increasing SwS trends in these regions may therefore have implications for flood hazards.

Spatial scale had long been a topic of conversation in snow hydrology as certain processes that occur at very small scales contribute to considerable within-grid cell heterogeneity as one scales up from point to grid cell to regional scales (Blöschl and



285 Sivapalan, 1995; Molotch and Bales, 2005). In this work, we find differences in the magnitude and timing of significant changes  
in  $SwS_A$  and  $SwS_M$  when we compare different spatial scales. For example, less of the US landscape shows significant changes  
in  $SwS_A$  in the ER3 analysis compared to the grid cell analysis. Thus, the aggregation of  $SwS_A$  into ER3s negates some of the  
grid cell-scale spatial  $SwS_A$  trends. Temporally, there is a higher fraction of sites with a significant positive increase in  $SwS_M$   
from October - March in the grid cell analysis compared to the ER3 analysis. This indicates that local significant increases in  
290  $SwS_M$  at grid cell scales are negated by smaller magnitude increases in  $SwS_M$  or decreases in  $SwS_M$  at many locations once the  
 $SwS_M$  is aggregated to ER3 scales. From a water resources perspective, these findings underscore the importance of choosing  
an appropriate aggregation scale in order to accomplish management goals.

Mountains play an out-sized role in natural reservoir storage on the US landscape. Across all mountain ER3s, there has  
been a 22% decline in  $SwS_A$  over the 39 year period of study. In the western US, where snowmelt is vital to supplementing  
295 warm-season water supplies, about 70% of runoff in mountainous regions originates as snow (Li et al., 2017). The ER3  
mountain ranges considered in this work include the headwaters to 13 of the 18 water basins located in the US, underscoring  
the importance of these natural reservoirs to water resources. The loss of  $SwS$  in these regions is of further concern as the  
warm season is projected to increase in length due to anthropogenic climate warming (Mallakpour et al., 2018; Padrón et al.,  
2020). Furthermore, it is possible that natural variability has in fact slowed the decline of western snowpacks since the 1980s,  
300 suggesting that snow declines may accelerate once the current natural climate mode changes (Siler et al., 2019). Overall, the  
capacity of natural snow reservoirs is declining in most of the western US and across most mountain ranges in the US. Because  
of this, monitoring our natural snow reservoirs is essential. Metrics like  $SwS$  are highly flexible in space and time and can be  
used in monitoring change and evaluating future projections.

$SwS_A$ , the changes in  $SwS_A$ , and the variability in  $SwS_D$  are all influenced by elevation. The greatest amount of snow water  
305 storage occurs on a disproportionately small fraction of our landscape - at the highest elevations of mountain ER3s. Almost all  
mountainous ER3s are losing  $SwS_A$  at all elevations. In the majority of mountain ER3s, the highest elevations have experienced  
the greatest losses  $SwS_A$  over the last 49 years. The elevation-dependent changes in our natural snow reservoirs are likely as-  
sociated to documented elevation-dependant changes in temperature and precipitation (Wang et al., 2014; Harpold et al., 2012;  
Pepin et al., 2015, 2022; Qixiang et al., 2018). Winter temperature have increased significantly in the recent past (Vose et al.,  
310 2017), which increases the vapor pressure deficit in the atmosphere and may enhance sublimation and vapor fluxes Harpold  
et al. (2012). Higher elevations have also warmed at faster rates than their low elevation counterparts, where there have been  
increasing trends in precipitation (Wang et al., 2014; Pepin et al., 2022). Wang et al. (2014) suggests that elevational warming  
amplification is likely associated with effective moisture convection. These mechanistic driver are a plausible explanation for  
finding the greatest  $SwS_A$  loss at the highest elevations.

315 This work also finds elevation-dependant changes in  $SwS_D$  variability. Assuming there have not been systematic changes  
in synoptic weather patterns,  $SwS_D$  variability has likely increased as a result of winter freezing levels moving to higher  
elevations (Catalano et al., 2019), an increased fraction of precipitation falling as rain instead of snow and more rain falling  
on snow (McCabe et al., 2007) - all of which are related to increasing winter temperatures. Decreases in  $SwS_D$  variability at  
higher elevations, where there are declining trends in  $SwS_A$ , may be a result of shallower snowpacks overall.



320 Comparison of the various snow metrics provides insight as to how the SWE curve is changing. Since April 1st SWE is largely used as standard time to capture an estimate of  $SWE_{max}$  in a way that is uniform across stations, and since the percent change in April 1st SWE nearly identical to the percent change in  $SWE_{max}$ , this discussion will focus on the relationship between  $SWE_{max}$ , SCD and SwS. Starting with the conceptual SWE curve illustrated in figure 1a, the area of the  $SwS_A$  triangle is;

$$325 \quad SwS_A = \frac{1}{2} SWE_{max} SCD. \quad (2)$$

If the geometry of the conceptual SWE were to be preserved over time, the SWE curve would be uniformly scaled and we would expect the percent change in  $SWE_{max}$  and the percent change in SCD to be equal, i.e.,

$$\frac{d(SWE_{max})}{SWE_{max}} = \frac{d(SCD)}{SCD}. \quad (3)$$

Additionally, the percent change in SwS would equal the sum of these

$$330 \quad \frac{d(SwS)}{SwS} = \frac{d(SWE_{max})}{SWE_{max}} + \frac{d(SCD)}{SCD}. \quad (4)$$

In this scenario, we would expect the percent change in  $SWE_{max}$  or SCD to be half the percent change in SwS. However, the regression plots in figure 11 reveal that

$$\frac{d(SCD)}{SCD} = 0.26 \frac{d(SwS)}{SwS} \quad (5)$$

and

$$335 \quad \frac{d(SWE_{max})}{SWE_{max}} = 0.85 \frac{d(SwS)}{SwS}. \quad (6)$$

This means that the  $SWE_{max}$  is decreasing faster than SCD. Thus, we find that the conceptual SWE curve has been flattening over the 39-year period of record.

The conceptual SWE curve and the above discussion is focused on a typical mountain snow pack, with a distinct period of steady accumulation up to a  $SWE_{max}$ , followed by a similarly steady ablation season. While mountain snowpacks play a key role in natural water storage, other types of snowpacks also have distinct characteristics and are important to the hydrological cycle. For example, ephemeral snowpacks play a role in soil moisture and runoff regimes (Livneh and Badger, 2020; Hamlet and Lettenmaier, 2007) and experience accumulation and ablation processes nearly in tandem (Liston and Elder, 2006). Ephemeral snowpacks tend to have a lower cold content than mountain snowpacks and come and go throughout the winter (Sturm et al., 1995; Hatchett, 2021). Alternatively, Greenland and Antarctic ice sheets generally only experience accumulation processes (Liston and Elder, 2006). Because of the transient nature of ephemeral snowpacks or the lack of an ablation season on ice sheets, metrics such as April 1 SWE,  $SWE_{max}$  and SCD may not be relevant. These scenarios are examples of where a more flexible metric, such as SwS, could be employed to characterize the annual (or other timescale) storage across a variety of snowpack types, which could be beneficial for universal monitoring of snow.



## 5 Conclusions

350 In this paper, SwS is used to identify where and to what extent water storage in natural snow reservoirs has already changed in the observational record. Mountains, especially western mountains, play an inordinate role in natural water storage relative to the surrounding landscape. These high-elevation natural snow reservoirs are responsible for the greatest SwS<sub>A</sub>, and have generally experienced the greatest declines in SwS<sub>A</sub>. Declines SwS<sub>A</sub> are associated with a fundamental shift in the shape of the SWE-curve as it appears to be flattening. As we move into a future of increased snow variability, diminished snowpacks  
355 and as more of the winter snow landscape transitions to ephemeral regimes, temporally static metrics such as April 1 SWE and SWE<sub>max</sub> may become less representative of our snowpacks and it may be valuable to have metrics such as SwS that can adapt to a wide range of circumstances. Spatially and temporally flexible metrics such as SwS may become increasingly valuable particularly when it comes to monitoring change.

Declining storage in our natural snow reservoirs has broad implications for human and ecological systems. Natural snow  
360 reservoirs help to increase water storage far beyond the capacity of man-made reservoirs in the western US, supporting their roll in linking cool-season precipitation to warm-season water demand. As one of the most robust projected impacts of climate change is a continued increase in air temperatures, it is likely that declining trends in SwS<sub>A</sub> will continue. Water managers, planners and decision makers will need to account for these declines in natural snow water storage as they relate to streamflows for fish migration and recreation, municipal and agricultural water supplies and flood hazards. Though this paper does not  
365 focus on future predictions of snowpack, SwS could be a useful tool for understanding how our natural snow reservoirs change in the future.

*Data availability.* Below is an enumerated list providing links to the publicly available datasets used in this study.

1. SnoTel (<https://wcc.sc.egov.usda.gov/reportGenerator/>)
2. UASWE (<https://nsidc.org/data/nsidc-0719/versions/1>)
- 370 3. NASA SRTM (<https://lpdaac.usgs.gov/products/srtmgl1v003/>)
4. USGS WBD (<https://datagateway.nrcs.usda.gov>)
5. EPA Ecoregions (<https://www.epa.gov/eco-research/level-iii-and-iv-ecoregions-continental-united-states>)

*Author contributions.* CMA and DFH designed the research questions. CMA determined the methodology and conducted the analysis. DFH conceptualized the SwS metric. CMA prepared the paper, with guidance and feedback from DFH.

375 *Competing interests.* The authors declare that they have no competing interests.

<https://doi.org/10.5194/egusphere-2023-596>

Preprint. Discussion started: 30 May 2023

© Author(s) 2023. CC BY 4.0 License.



*Acknowledgements.* This work was made supported by funding from the Graduate School Oregon Lottery Award for Academic Excellence from Oregon State University and the Alumni Award from the Water Resources Graduate Program at Oregon State University. We thank P.C. Loikith and L.R. Hawkins for their contributions to this research.



## References

- 380 Barnett, T. P., Adam, J. C., and Lettenmaier, D. P.: Potential impacts of a warming climate on water availability in snow-dominated regions, *Nature*, 438, 303–309, <https://doi.org/10.1038/nature04141>, bandiera\_abtest: a Cg\_type: Nature Research Journals Number: 7066 Primary\_atype: Reviews Publisher: Nature Publishing Group, 2005.
- Blöschl, G. and Sivapalan, M.: Scale issues in hydrological modelling: A review, *Hydrological Processes*, 9, 251–290, <https://doi.org/10.1002/hyp.3360090305>, \_eprint: <https://onlinelibrary.wiley.com/doi/pdf/10.1002/hyp.3360090305>, 1995.
- 385 Boon, S.: Snow accumulation and ablation in a beetle-killed pine stand in Northern Interior British Columbia, *Journal of Ecosystems and Management*, <https://doi.org/10.22230/jem.2007v8n3a369>, 2007.
- Bormann, K. J., Brown, R. D., Derksen, C., and Painter, T. H.: Estimating snow-cover trends from space, *Nature Climate Change*, 8, 924–928, <https://doi.org/10.1038/s41558-018-0318-3>, number: 11 Publisher: Nature Publishing Group, 2018.
- Broxton, P., Zeng, X., and Dawson, N.: Daily 4 km Gridded SWE and Snow Depth from Assimilated In-Situ and Modeled  
390 Data over the Conterminous US, Version 1, NASA National Snow and Ice Data Center Distributed Active Archive Center, <https://doi.org/https://doi.org/10.5067/0GGPB220EX6A>, 2019.
- Catalano, A. J., Loikith, P. C., and Aragon, C. M.: Spatiotemporal Variability of Twenty-First-Century Changes in Site-Specific Snowfall Frequency Over the Northwest United States, *Geophysical Research Letters*, 46, 10 122–10 131, <https://doi.org/10.1029/2019GL084401>, \_eprint: <https://onlinelibrary.wiley.com/doi/pdf/10.1029/2019GL084401>, 2019.
- 395 Center, N. O. H. R. S.: Snow Data Assimilation System (SNODAS) Data Products at NSIDC, Version 1., NSIDC: National Snow and Ice Data Center, <https://doi.org/https://doi.org/10.7265/N5TB14TC>, 2004.
- Choi, G., Robinson, D. A., and Kang, S.: Changing Northern Hemisphere Snow Seasons, *Journal of Climate*, 23, 5305–5310, <https://doi.org/10.1175/2010JCLI3644.1>, publisher: American Meteorological Society Section: *Journal of Climate*, 2010.
- Clow, D. W.: Changes in the Timing of Snowmelt and Streamflow in Colorado: A Response to Recent Warming, *Journal of Climate*, 23,  
400 2293–2306, <https://doi.org/10.1175/2009JCLI2951.1>, publisher: American Meteorological Society Section: *Journal of Climate*, 2010.
- Collins, M. J.: Evidence for Changing Flood Risk in New England Since the Late 20th Century<sup>1</sup>, *JAWRA Journal of the American Water Resources Association*, 45, 279–290, <https://doi.org/10.1111/j.1752-1688.2008.00277.x>, \_eprint: <https://onlinelibrary.wiley.com/doi/pdf/10.1111/j.1752-1688.2008.00277.x>, 2009.
- Daly, C., Halbleib, M., Smith, J. I., Gibson, W. P., Doggett, M. K., Taylor, G. H., Curtis, J., and Pasteris, P. P.: Physiographically sensitive  
405 mapping of climatological temperature and precipitation across the conterminous United States, *International Journal of Climatology*, 28, 2031–2064, <https://doi.org/10.1002/joc.1688>, \_eprint: <https://onlinelibrary.wiley.com/doi/pdf/10.1002/joc.1688>, 2008.
- Dawson, N., Broxton, P., and Zeng, X.: Evaluation of Remotely Sensed Snow Water Equivalent and Snow Cover Extent over the Contiguous United States, *Journal of Hydrometeorology*, 19, 1777–1791, <https://doi.org/10.1175/JHM-D-18-0007.1>, publisher: American Meteorological Society Section: *Journal of Hydrometeorology*, 2018.
- 410 Derksen, C. and Brown, R.: Spring snow cover extent reductions in the 2008–2012 period exceeding climate model projections, *Geophysical Research Letters*, 39, <https://doi.org/10.1029/2012GL053387>, \_eprint: <https://onlinelibrary.wiley.com/doi/pdf/10.1029/2012GL053387>, 2012.
- Easterling, D., Arnold, J., Knutson, T., Kunkel, K., LeGrande, A., Leung, L., Vose, R., Waliser, D., and Wehner, M.: Ch. 7: Precipitation Change in the United States. Climate Science Special Report: Fourth National Climate Assessment, Volume I, Tech. rep., U.S. Global  
415 Change Research Program, <https://doi.org/10.7930/J0H993CC>, 2017.



- Farr, T. G., Rosen, P. A., Caro, E., Crippen, R., Duren, R., Hensley, S., Kobrick, M., Paller, M., Rodriguez, E., Roth, L., Seal, D., Shaffer, S., Shimada, J., Umland, J., Werner, M., Oskin, M., Burbank, D., and Alsdorf, D.: The Shuttle Radar Topography Mission, *Reviews of Geophysics*, 45, <https://doi.org/10.1029/2005RG000183>, \_eprint: <https://onlinelibrary.wiley.com/doi/pdf/10.1029/2005RG000183>, 2007.
- 420 Gleason, K. E., McConnell, J. R., Arienzo, M. M., Chellman, N., and Calvin, W. M.: Four-fold increase in solar forcing on snow in western U.S. burned forests since 1999, *Nature Communications*, 10, 2026, <https://doi.org/10.1038/s41467-019-09935-y>, number: 1 Publisher: Nature Publishing Group, 2019.
- Hamed, K. and Rao, A.: A modified Mann-Kendall trend test for autocorrelated data, *Journal of Hydrology*, 204, 182–196, [https://doi.org/10.1016/S0022-1694\(97\)00125-X](https://doi.org/10.1016/S0022-1694(97)00125-X), publisher: Elsevier, 1998.
- Hamlet, A. F. and Lettenmaier, D. P.: Effects of 20th century warming and climate variability on flood risk in the western U.S., *Water Resources Research*, 43, <https://doi.org/10.1029/2006WR005099>, \_eprint: <https://onlinelibrary.wiley.com/doi/pdf/10.1029/2006WR005099>, 2007.
- 425 Hamlet, A. F., Mote, P. W., Clark, M. P., and Lettenmaier, D. P.: Effects of Temperature and Precipitation Variability on Snowpack Trends in the Western United States, *Journal of Climate*, 18, 4545–4561, <https://doi.org/10.1175/JCLI3538.1>, publisher: American Meteorological Society Section: *Journal of Climate*, 2005.
- 430 Harpold, A., Brooks, P., Rajagopal, S., Heidebuchel, I., Jardine, A., and Stielstra, C.: Changes in snowpack accumulation and ablation in the intermountain west, *Water Resources Research*, 48, <https://doi.org/10.1029/2012WR011949>, \_eprint: <https://onlinelibrary.wiley.com/doi/pdf/10.1029/2012WR011949>, 2012.
- Hatchett, B. J.: Seasonal and Ephemeral Snowpacks of the Conterminous United States, *Hydrology*, 8, 32, <https://doi.org/10.3390/hydrology8010032>, number: 1 Publisher: Multidisciplinary Digital Publishing Institute, 2021.
- 435 Hirsch, R. M., Slack, J. R., and Smith, R. A.: Techniques of trend analysis for monthly water quality data, *Water Resources Research*, 18, 107–121, <https://doi.org/10.1029/WR018i001p00107>, \_eprint: <https://onlinelibrary.wiley.com/doi/pdf/10.1029/WR018i001p00107>, 1982.
- Huning, L. S. and AghaKouchak, A.: Mountain snowpack response to different levels of warming, *Proceedings of the National Academy of Sciences*, 115, 10932–10937, <https://doi.org/10.1073/pnas.1805953115>, 2018.
- Hussain, M. and Mahmud, I.: pyMannKendall: a python package for non parametric Mann Kendall family of trend tests., *Journal of Open Source Software*, 4, 1556, <https://doi.org/10.21105/joss.01556>, 2019.
- 440 Immerzeel, W. W., Lutz, A. F., Andrade, M., Bahl, A., Biemans, H., Bolch, T., Hyde, S., Brumby, S., Davies, B. J., Elmore, A. C., Emmer, A., Feng, M., Fernández, A., Haritashya, U., Kargel, J. S., Koppes, M., Kraaijenbrink, P. D. A., Kulkarni, A. V., Mayewski, P. A., Nepal, S., Pacheco, P., Painter, T. H., Pellicciotti, F., Rajaram, H., Rupper, S., Sinisalo, A., Shrestha, A. B., Viviroli, D., Wada, Y., Xiao, C., Yao, T., and Baillie, J. E. M.: Importance and vulnerability of the world’s water towers, *Nature*, 577, 364–369, <https://doi.org/10.1038/s41586-019-1822-y>, 2020.
- Krogh, S. A., Broxton, P. D., Manley, P. N., and Harpold, A. A.: Using Process Based Snow Modeling and Lidar to Predict the Effects of Forest Thinning on the Northern Sierra Nevada Snowpack, *Frontiers in Forests and Global Change*, 3, <https://www.frontiersin.org/articles/10.3389/ffgc.2020.00021>, 2020.
- 450 Li, D., Wrzesien, M. L., Durand, M., Adam, J., and Lettenmaier, D. P.: How much runoff originates as snow in the western United States, and how will that change in the future?, *Geophysical Research Letters*, 44, 6163–6172, <https://doi.org/10.1002/2017GL073551>, \_eprint: <https://onlinelibrary.wiley.com/doi/pdf/10.1002/2017GL073551>, 2017.
- Liston, G. E. and Elder, K.: A Distributed Snow-Evolution Modeling System (SnowModel), *Journal of Hydrometeorology*, 7, 1259–1276, <https://doi.org/10.1175/JHM548.1>, publisher: American Meteorological Society Section: *Journal of Hydrometeorology*, 2006.



- Livneh, B. and Badger, A. M.: Drought less predictable under declining future snowpack, *Nature Climate Change*, 10, 452–458, <https://doi.org/10.1038/s41558-020-0754-8>, number: 5 Publisher: Nature Publishing Group, 2020.
- Lute, A. C., Abatzoglou, J. T., and Hegewisch, K. C.: Projected changes in snowfall extremes and interannual variability of snowfall in the western United States, *Water Resources Research*, 51, 960–972, <https://doi.org/10.1002/2014WR016267>, \_eprint: <https://onlinelibrary.wiley.com/doi/pdf/10.1002/2014WR016267>, 2015.
- Mallakpour, I., Sadegh, M., and AghaKouchak, A.: A new normal for streamflow in California in a warming climate: Wetter wet seasons and drier dry seasons, *Journal of Hydrology*, 567, 203–211, <https://doi.org/10.1016/j.jhydrol.2018.10.023>, 2018.
- McCabe, G. J., Clark, M. P., and Hay, L. E.: Rain-on-Snow Events in the Western United States, *Bulletin of the American Meteorological Society*, 88, 319–328, <https://doi.org/10.1175/BAMS-88-3-319>, publisher: American Meteorological Society Section: Bulletin of the American Meteorological Society, 2007.
- McMAHON, G., GREGONIS, S. M., WALTMAN, S. W., OMERNIK, J. M., THORSON, T. D., FREEOUF, J. A., RORICK, A. H., and KEYS, J. E.: Developing a Spatial Framework of Common Ecological Regions for the Conterminous United States, *Environmental Management*, 28, 293–316, <https://doi.org/10.1007/s0026702429>, 2001.
- Molotch, N. P. and Bales, R. C.: Scaling snow observations from the point to the grid element: Implications for observation network design, *Water Resources Research*, 41, <https://doi.org/10.1029/2005WR004229>, \_eprint: <https://onlinelibrary.wiley.com/doi/pdf/10.1029/2005WR004229>, 2005.
- Mote, P. W., Li, S., Lettenmaier, D. P., Xiao, M., and Engel, R.: Dramatic declines in snowpack in the western US, *npj Climate and Atmospheric Science*, 1, 1–6, <https://doi.org/10.1038/s41612-018-0012-1>, number: 1 Publisher: Nature Publishing Group, 2018.
- Musselman, K. N., Addor, N., Vano, J. A., and Molotch, N. P.: Winter melt trends portend widespread declines in snow water resources, *Nature Climate Change*, 11, 418–424, <https://doi.org/10.1038/s41558-021-01014-9>, number: 5 Publisher: Nature Publishing Group, 2021.
- Nolin, A. W., Sproles, E. A., Rupp, D. E., Crumley, R. L., Webb, M. J., Palomaki, R. T., and Mar, E.: New snow metrics for a warming world, *Hydrological Processes*, 35, e14262, <https://doi.org/10.1002/hyp.14262>, \_eprint: <https://onlinelibrary.wiley.com/doi/pdf/10.1002/hyp.14262>, 2021.
- Notarnicola, C.: Hotspots of snow cover changes in global mountain regions over 2000–2018, *Remote Sensing of Environment*, 243, 111781, <https://doi.org/10.1016/j.rse.2020.111781>, 2020.
- Novotny, E. V. and Stefan, H. G.: Stream flow in Minnesota: Indicator of climate change, *Journal of Hydrology*, 334, 319–333, <https://doi.org/10.1016/j.jhydrol.2006.10.011>, 2007.
- Olsen, J. R., Stedinger, J. R., Matalas, N. C., and Stakhiv, E. Z.: Climate Variability and Flood Frequency Estimation for the Upper Mississippi and Lower Missouri Rivers<sup>1</sup>, *JAWRA Journal of the American Water Resources Association*, 35, 1509–1523, <https://doi.org/10.1111/j.1752-1688.1999.tb04234.x>, \_eprint: <https://onlinelibrary.wiley.com/doi/pdf/10.1111/j.1752-1688.1999.tb04234.x>, 1999.
- Omernik, J. M. and Griffith, G. E.: Ecoregions of the Conterminous United States: Evolution of a Hierarchical Spatial Framework, *Environmental Management*, 54, 1249–1266, <https://doi.org/10.1007/s00267-014-0364-1>, 2014.
- Padrón, R. S., Gudmundsson, L., Decharme, B., Ducharme, A., Lawrence, D. M., Mao, J., Peano, D., Krinner, G., Kim, H., and Seneviratne, S. I.: Observed changes in dry-season water availability attributed to human-induced climate change, *Nature Geoscience*, 13, 477–481, <https://doi.org/10.1038/s41561-020-0594-1>, number: 7 Publisher: Nature Publishing Group, 2020.





- 490 Pederson, G. T., Betancourt, J. L., and McCabe, G. J.: Regional patterns and proximal causes of the recent snowpack decline in the Rocky Mountains, U.S., *Geophysical Research Letters*, 40, 1811–1816, <https://doi.org/10.1002/grl.50424>, <https://onlinelibrary.wiley.com/doi/pdf/10.1002/grl.50424>, 2013.
- Pepin, N., Bradley, R. S., Diaz, H. F., Baraer, M., Caceres, E. B., Forsythe, N., Fowler, H., Greenwood, G., Hashmi, M. Z., Liu, X. D., Miller, J. R., Ning, L., Ohmura, A., Palazzi, E., Rangwala, I., Schöner, W., Severskiy, I., Shahgedanova, M., Wang, M. B., Williamson, S. N.,  
495 Yang, D. Q., and Mountain Research Initiative EDW Working Group: Elevation-dependent warming in mountain regions of the world, *Nature Climate Change*, 5, 424–430, <https://doi.org/10.1038/nclimate2563>, number: 5 Publisher: Nature Publishing Group, 2015.
- Pepin, N. C., Arnone, E., Gobiet, A., Haslinger, K., Kotlarski, S., Notarnicola, C., Palazzi, E., Seibert, P., Serafin, S., Schöner, W., Terzago, S., Thornton, J. M., Vuille, M., and Adler, C.: Climate Changes and Their Elevational Patterns in the Mountains of the World, *Reviews of Geophysics*, 60, e2020RG000730, <https://doi.org/10.1029/2020RG000730>, <https://onlinelibrary.wiley.com/doi/pdf/10.1029/2020RG000730>,  
500 <https://onlinelibrary.wiley.com/doi/pdf/10.1029/2020RG000730>, 2022.
- Pugh, E. and Small, E.: The impact of pine beetle infestation on snow accumulation and melt in the headwaters of the Colorado River, *Ecohydrology*, 5, 467–477, <https://doi.org/10.1002/eco.239>, [eprint: https://onlinelibrary.wiley.com/doi/pdf/10.1002/eco.239](https://onlinelibrary.wiley.com/doi/pdf/10.1002/eco.239), 2012.
- Qixiang, W., Wang, M., and Fan, X.: Seasonal patterns of warming amplification of high-elevation stations across the globe, *International Journal of Climatology*, 38, 3466–3473, <https://doi.org/10.1002/joc.5509>, <https://onlinelibrary.wiley.com/doi/pdf/10.1002/joc.5509>,  
505 <https://onlinelibrary.wiley.com/doi/pdf/10.1002/joc.5509>, 2018.
- Rupp, D. E., Mote, P. W., Bindoff, N. L., Stott, P. A., and Robinson, D. A.: Detection and Attribution of Observed Changes in Northern Hemisphere Spring Snow Cover, *Journal of Climate*, 26, 6904–6914, <https://doi.org/10.1175/JCLI-D-12-00563.1>, publisher: American Meteorological Society Section: *Journal of Climate*, 2013.
- Serreze, M. C., Clark, M. P., Armstrong, R. L., McGinnis, D. A., and Pulwarty, R. S.: Characteristics of the western United States snowpack from snowpack telemetry (SNO) data, *Water Resources Research*, 35, 2145–2160, <https://doi.org/10.1029/1999WR900090>, [eprint: https://onlinelibrary.wiley.com/doi/pdf/10.1029/1999WR900090](https://onlinelibrary.wiley.com/doi/pdf/10.1029/1999WR900090),  
510 <https://onlinelibrary.wiley.com/doi/pdf/10.1029/1999WR900090>, 1999.
- Siirila-Woodburn, E. R., Rhoades, A. M., Hatchett, B. J., Huning, L. S., Szinai, J., Tague, C., Nico, P. S., Feldman, D. R., Jones, A. D., Collins, W. D., and Kaatz, L.: A low-to-no snow future and its impacts on water resources in the western United States, *Nature Reviews Earth & Environment*, 2, 800–819, <https://doi.org/10.1038/s43017-021-00219-y>, number: 11 Publisher: Nature Publishing Group, 2021.
- 515 Siler, N., Proistosescu, C., and Po-Chedley, S.: Natural Variability Has Slowed the Decline in Western U.S. Snowpack Since the 1980s, *Geophysical Research Letters*, 46, 346–355, <https://doi.org/10.1029/2018GL081080>, [eprint: https://onlinelibrary.wiley.com/doi/pdf/10.1029/2018GL081080](https://onlinelibrary.wiley.com/doi/pdf/10.1029/2018GL081080),  
<https://onlinelibrary.wiley.com/doi/pdf/10.1029/2018GL081080>, 2019.
- Sturm, M., Holmgren, J., and Liston, G. E.: A Seasonal Snow Cover Classification System for Local to Global Applications, *Journal of Climate*, 8, 1261–1283, [https://doi.org/10.1175/1520-0442\(1995\)008<1261:ASSCCS>2.0.CO;2](https://doi.org/10.1175/1520-0442(1995)008<1261:ASSCCS>2.0.CO;2), publisher: American Meteorological Society Section: *Journal of Climate*, 1995.  
520
- Sturm, M., Goldstein, M. A., and Parr, C.: Water and life from snow: A trillion dollar science question, *Water Resources Research*, 53, 3534–3544, <https://doi.org/10.1002/2017WR020840>, [eprint: https://onlinelibrary.wiley.com/doi/pdf/10.1002/2017WR020840](https://onlinelibrary.wiley.com/doi/pdf/10.1002/2017WR020840), 2017.
- Sun, N., Yan, H., Wigmosta, M. S., Lundquist, J., Dickerson-Lange, S., and Zhou, T.: Forest Canopy Density Effects on Snowpack Across the Climate Gradients of the Western United States Mountain Ranges, *Water Resources Research*, 58, e2020WR029194, <https://doi.org/10.1029/2020WR029194>, [eprint: https://onlinelibrary.wiley.com/doi/pdf/10.1029/2020WR029194](https://onlinelibrary.wiley.com/doi/pdf/10.1029/2020WR029194),  
525 <https://doi.org/10.1029/2020WR029194>, <https://onlinelibrary.wiley.com/doi/pdf/10.1029/2020WR029194>, 2022.
- Troendle, C. A. and Reuss, J. O.: Effect of clear cutting on snow accumulation and water outflow at Fraser, Colorado, *Hydrology and Earth System Sciences*, 1, 325–332, <https://doi.org/10.5194/hess-1-325-1997>, publisher: Copernicus GmbH, 1997.



- Vose, R., Easterling, D., Kunkel, K., LeGrande, A., and Wehner, M.: Ch. 6: Temperature changes in the United States. In: Climate Science Special Report: Fourth National Climate Assessment, Volume I, Tech. rep., U.S. Global Change Research Program, Washington, DC, USA., 2017.
- 530
- Wang, Q., Fan, X., and Wang, M.: Recent warming amplification over high elevation regions across the globe, *Climate Dynamics*, 43, 87–101, <https://doi.org/10.1007/s00382-013-1889-3>, 2014.
- Wiel, K. v. d., Kapnick, S. B., Vecchi, G. A., Smith, J. A., Milly, P. C. D., and Jia, L.: 100-Year Lower Mississippi Floods in a Global Climate Model: Characteristics and Future Changes, *Journal of Hydrometeorology*, 19, 1547–1563, <https://doi.org/10.1175/JHM-D-18-0018.1>, publisher: American Meteorological Society Section: Journal of Hydrometeorology, 2018.
- 535
- Winkler, R., Boon, S., Zimonick, B., and Spittlehouse, D.: Snow accumulation and ablation response to changes in forest structure and snow surface albedo after attack by mountain pine beetle, *Hydrological Processes*, 28, 197–209, <https://doi.org/10.1002/hyp.9574>, \_eprint: <https://onlinelibrary.wiley.com/doi/pdf/10.1002/hyp.9574>, 2014.
- Winkler, R. D., Spittlehouse, D. L., and Golding, D. L.: Measured differences in snow accumulation and melt among clearcut, juvenile, and mature forests in southern British Columbia, *Hydrological Processes*, 19, 51–62, <https://doi.org/10.1002/hyp.5757>, \_eprint: <https://onlinelibrary.wiley.com/doi/pdf/10.1002/hyp.5757>, 2005.
- 540
- Zeng, X., Broxton, P., and Dawson, N.: Snowpack Change From 1982 to 2016 Over Conterminous United States, *Geophysical Research Letters*, 45, 12,940–12,947, <https://doi.org/10.1029/2018GL079621>, \_eprint: <https://onlinelibrary.wiley.com/doi/pdf/10.1029/2018GL079621>, 2018.

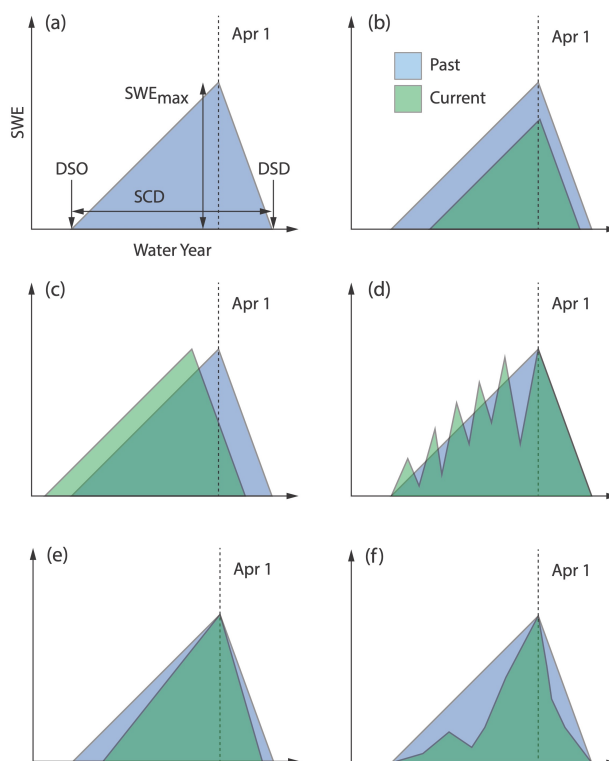


**Figure 1.** Theoretical SWE curves. Blue curves illustrate the past characteristic SWE curve and green curves demonstrate a range of ways the historic SWE curve may have changed.



**Table 1.** Summary of data used in this work.

Data set	Hosting agency	Data Type	Temporal resolution	Spatial resolution
Snow Telemetry (SnoTel)	Natural Resources Conservation Service (NRCS)	Point observations	Stations were selected with a period of record starting in water year 1982 and less than 10 percent of days missing	N/A
Cooperator Snow Sensors (COOP)	Natural Resources Conservation Service (NRCS)	Point observations	Stations were selected with a period of record starting in water year 1982 and less than 10 percent of days missing	N/A
University of Arizona SWE (UASWE)	National Snow and Ice Data Center (NSIDC)	Gridded product	water year 1982-present	4km x 4km
NASA SRTM Digital Elevation	Google Earth Engine (GEE)	Gridded product	N/A	30m x 30m
EPA Level III Ecoregions	Google Earth Engine (GEE)	Vector data	N/A	N/A

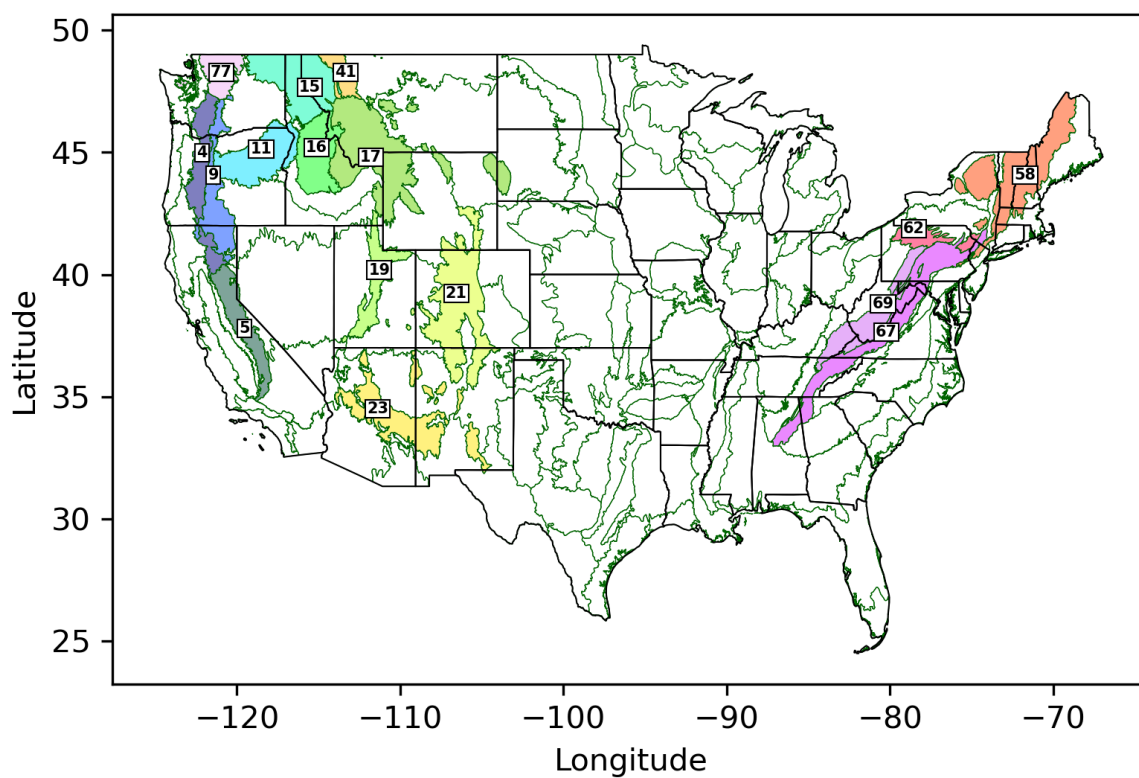


**Figure 2.** Map of ER3s in the US. Mountain ER3s are colorshaded and labeled.

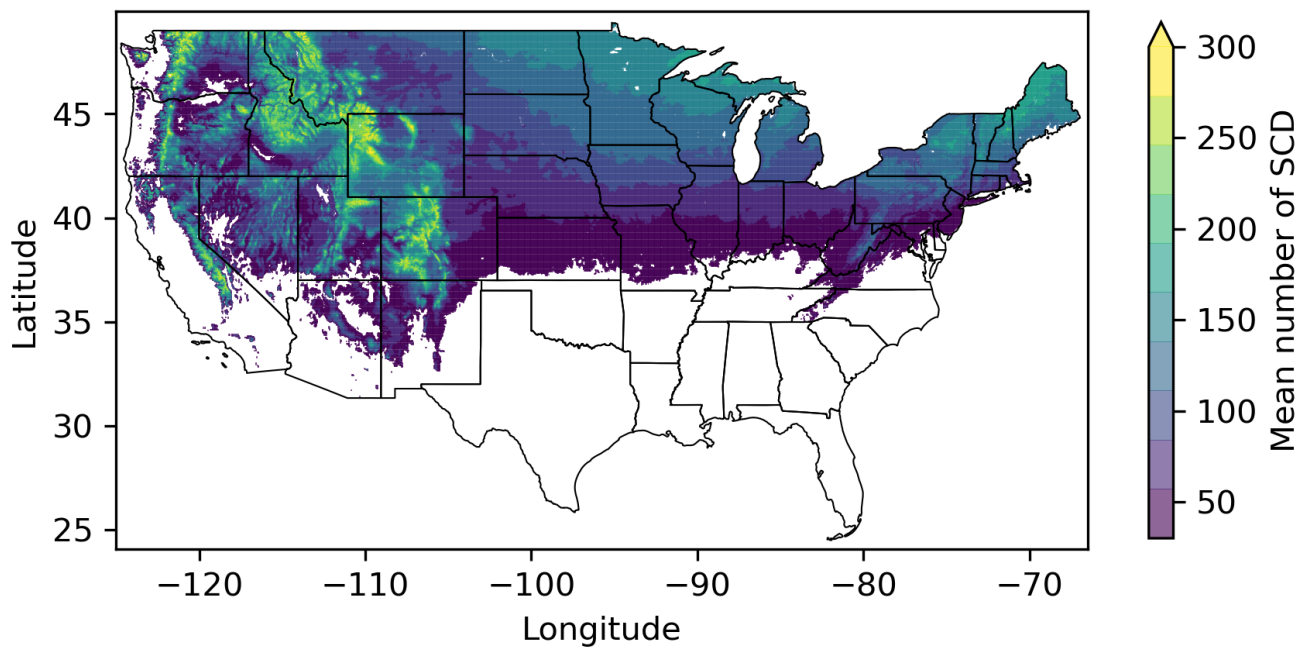


**Figure 3.** Study area indicated by color shading showing the mean number of annual SWE days across the contiguous US in locations that have a minimum average of 30 snow covered days/year over the period of record.

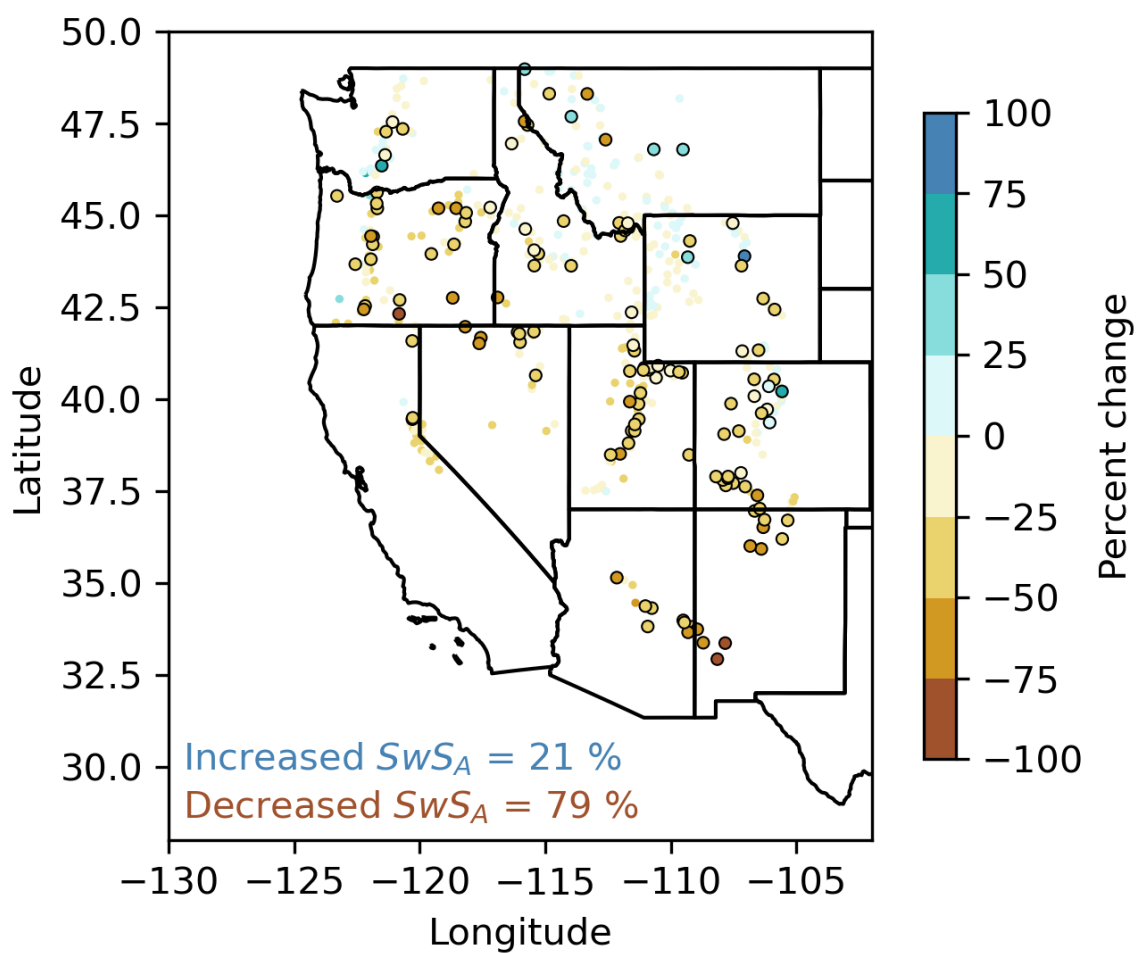


**Figure 4.** Percent change in  $SwS_A$  across US stations from water years 1982-2020. Large outlined circles indicate stations with  $p < 0.1$ .

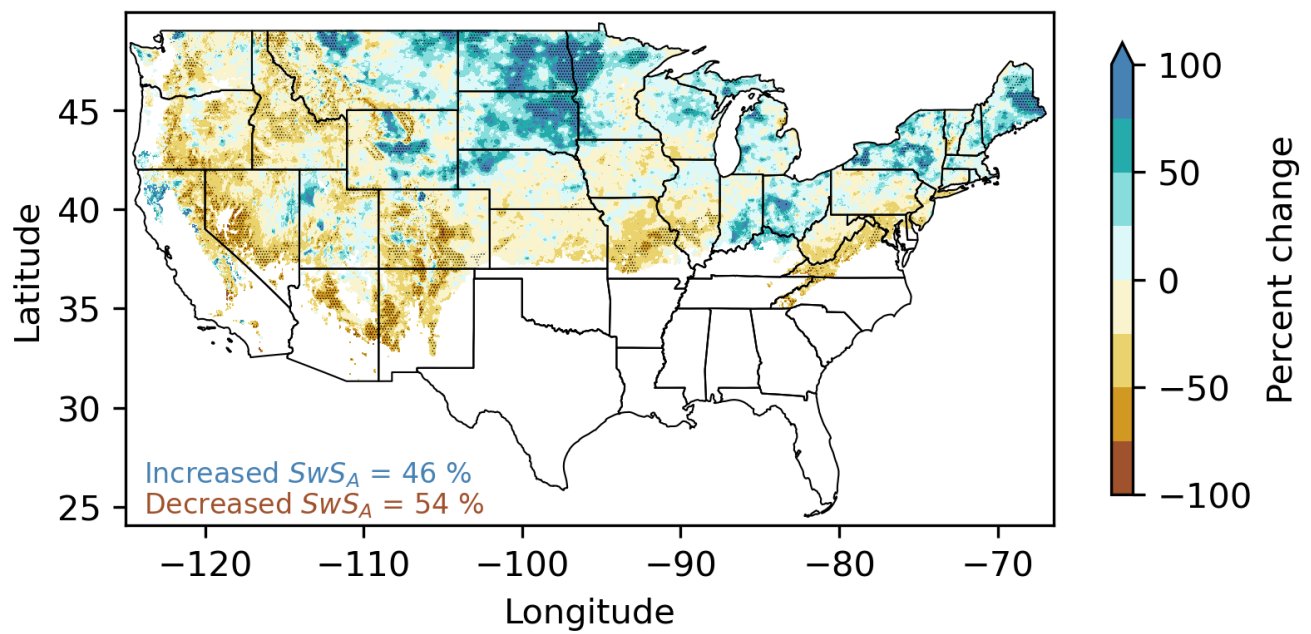


**Figure 5.** Grid cell-scale changes in  $SwS_A$  from water years 1982-2020 across the UASWE data set. Stippling indicates locations with  $p < 0.1$ .



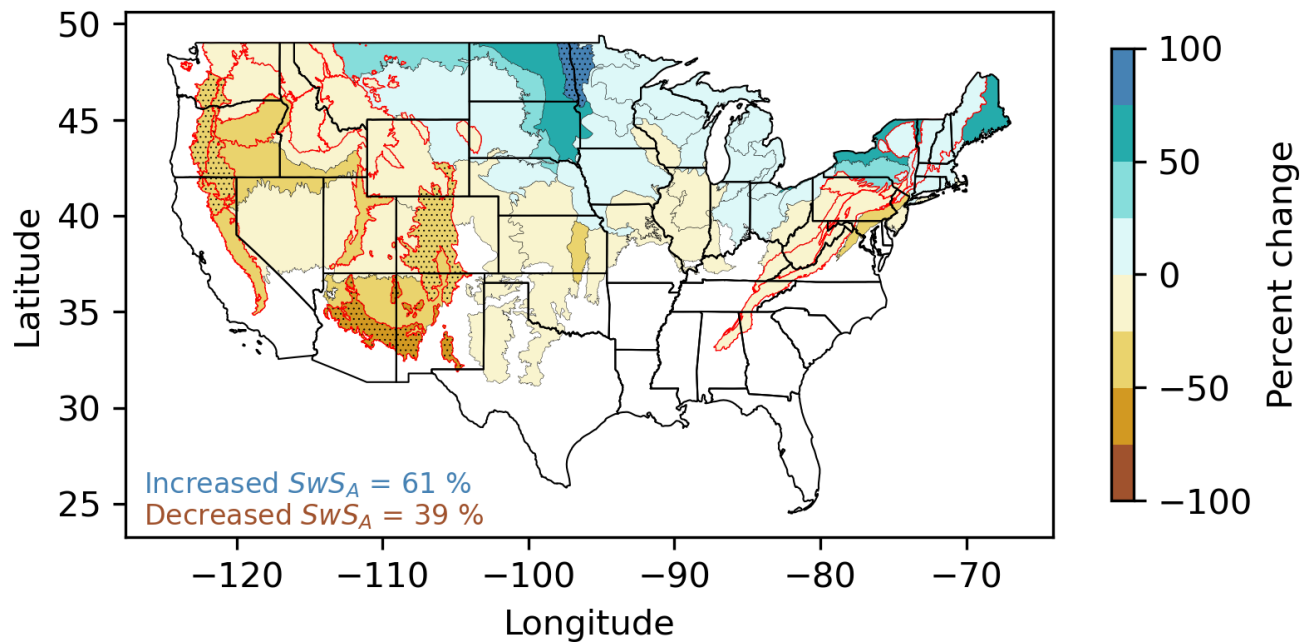


**Figure 6.** Grid cell-scale changes in  $SwS_A$  aggregated across ER3s from water years 1982-2020. Stippling indicates ER3s with  $p < 0.1$ .

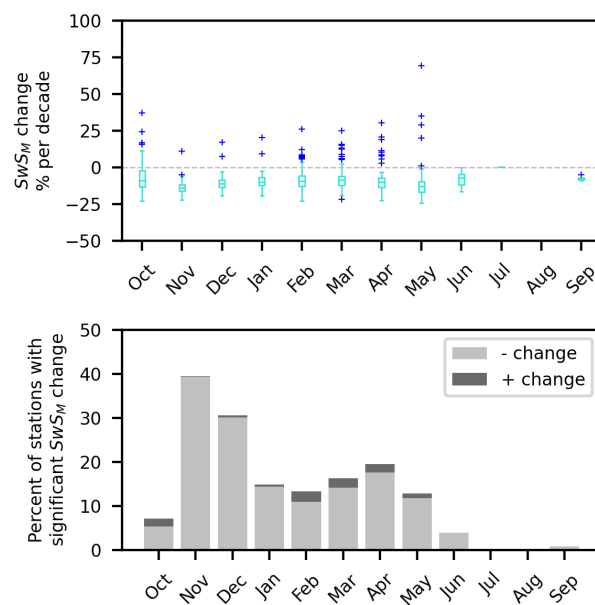


**Figure 7.** Percent change (significance  $p < 0.1$ ) in  $SWS_M$  across US stations. The top boxplot shows monthly percent change in snow water storage per decade. The rectangle indicates the interquartile range, with the middle bar indicating the median. The blue pluses are outlier points. The bottom bar chart shows the fraction of stations that had significant increases or decreases in SwS.

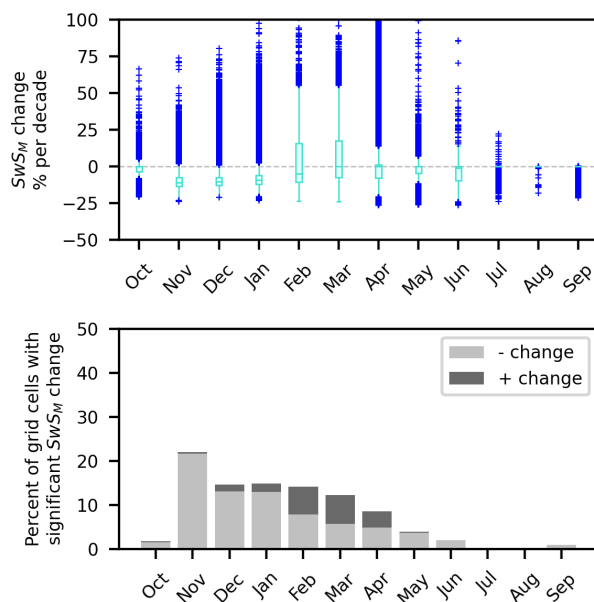


**Figure 8.** As in figure 7, but for the Grid cell-scale changes in SwS from water years 1982-2020 across the UASWE data set.

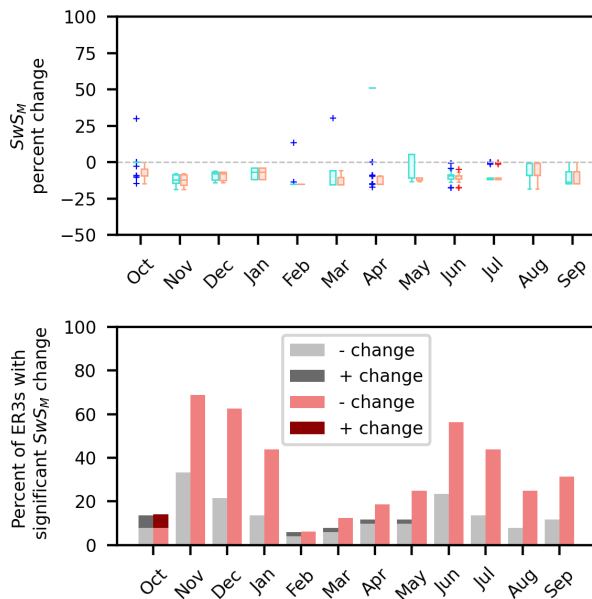


**Figure 9.** As in figure 7, but for changes in SwS aggregated across ER3s from water years 1982-2020. Red components of this figure indicate the results only considering mountain ER3s.



**Table 2.** Overview of SwS<sub>A</sub> in mountainous ER3s. Red p-values are significant at  $p < 0.1$ .

ER3 code and name	Average fraction of US SwS <sub>A</sub>	Percent change from 1982 to 2020	p-value
West			
4: Cascades	0.078	-39.02	0.08
5: Sierra Nevada	0.036	-37.74	0.23
9: Eastern Cascade Slopes and Foothills	0.023	-39.63	0.09
11: Blue Mountains	0.034	-25.58	0.16
15: Northern Rockies	0.08	-24.8	0.15
16: Idaho Batholith	0.083	-22.33	0.16
17: Middle Rockies	0.116	-18.68	0.19
19: Wasatch and Uinta Mountains	0.032	-29.14	0.14
21: Southern Rockies	0.098	-33.49	0.02
23: Arizona/New Mexico Mountains	0.009	-56.22	0.02
41: Canadian Rockies	0.039	-12.72	0.33
77: North Cascades	0.072	13.15	0.68
East			
58: Northeastern Highlands	0.035	13.15	0.68
62: North Central Appalachians	0.002	-2.38	0.94
67: Ridge and Valley	0.002	-11.48	0.73
69: Central Appalachians	0.003	-9.78	0.68

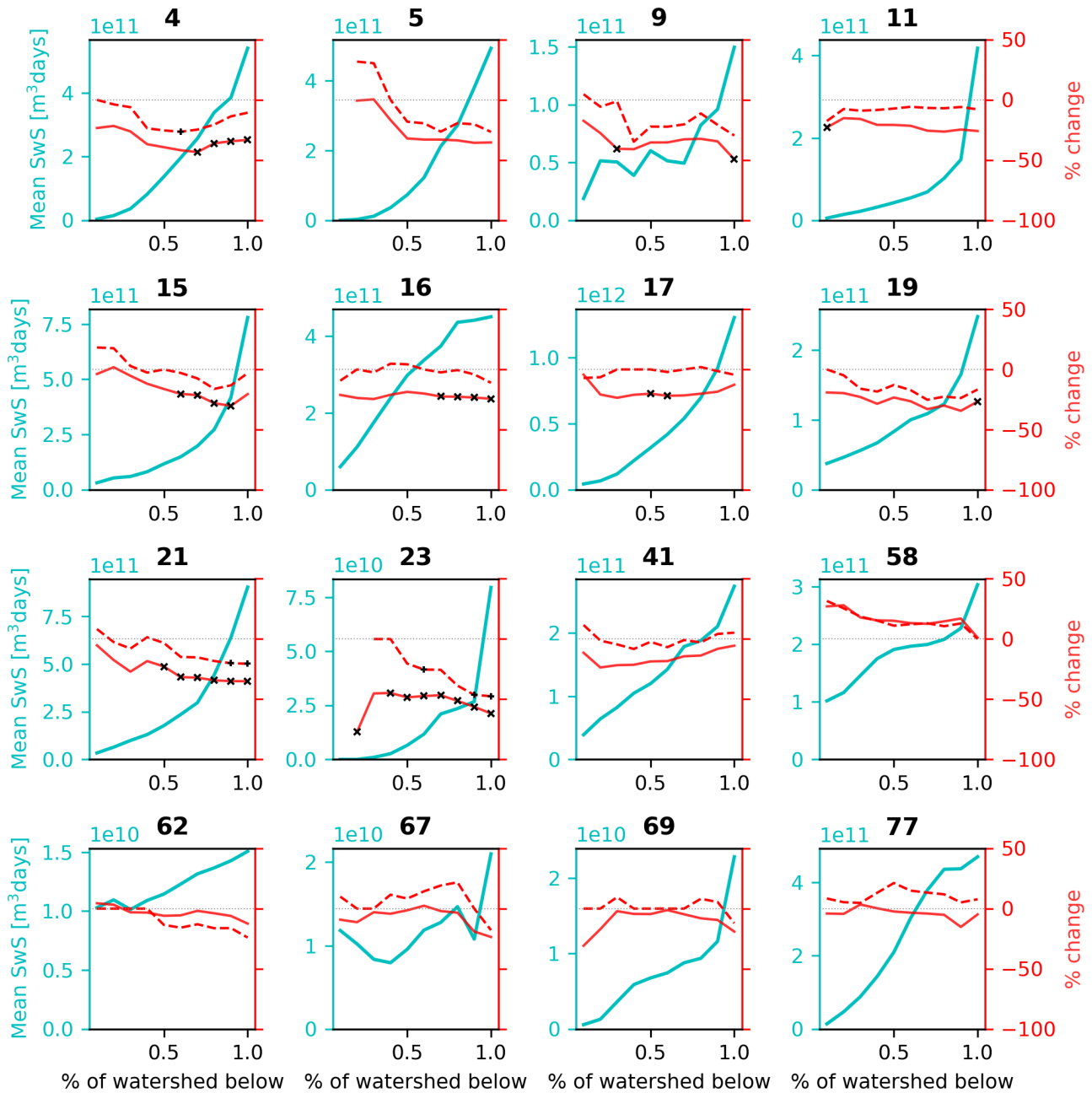


**Figure 10.**  $S_{wS_A}$  in each ER3 as a function of ER3 hypsometry. Teal line indicates the average  $A$  in each hypsometry bin from water years 1982-2020 (left axis). Solid red line indicates the percent change in  $A$  as a function of hypsometry for each mountain ER3 over the time period of interest (right axis). Black × symbols indicate where the percent change in  $S_{wS_A}$  is significant ( $p < 0.1$ ). Dashed red line indicates the percent change in the IQR of daily  $S_{wS}$  (aka daily SWE) as a function of hypsometry in each mountain ER3 over the time period of interest (right axis). Black + symbols indicate where the percent change in the IQR is significant ( $p < 0.1$ ).



**Table 3.** Summary of snow metric trends for water years 1982-2020.

Metric	Percent of stations with positive trend	Percent of stations with significant positive trend	Percent of stations with negative trend	Percent of stations with significant negative trend
SwS	21	2	79	21
SCD	14	1	79	29
SWE <sub>max</sub>	23	2	74	23
Day of SWE <sub>max</sub>	28	2	61	15
April 1 SWE	24	2	68	22

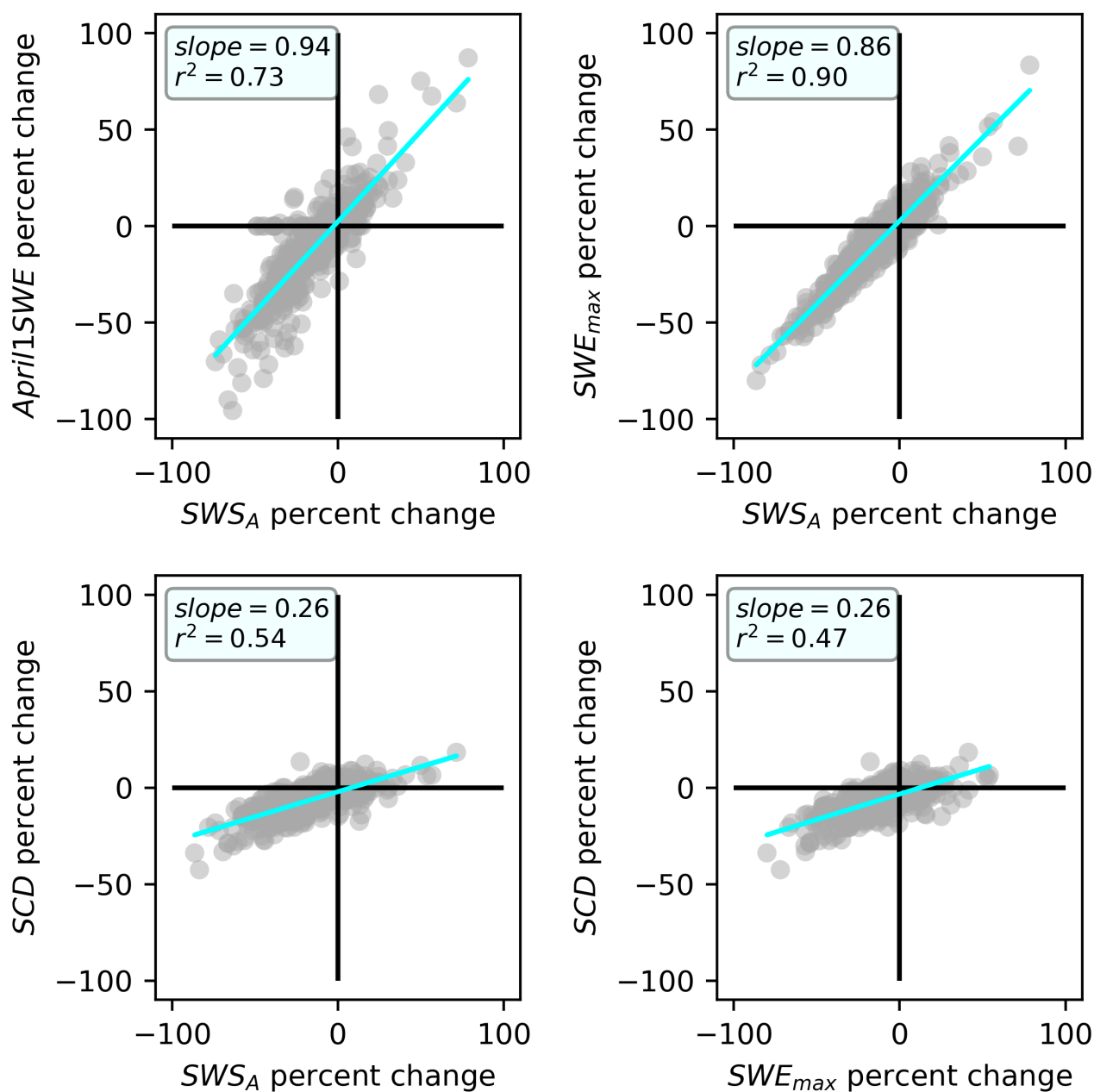


**Figure 11.** Regression of percent change in  $SwS_A$  with percent change in April 1 SWE (top left),  $SWE_{max}$  (top right) and SCD (bottom left). Regression of  $SWE_{max}$  with SCD (bottom right).